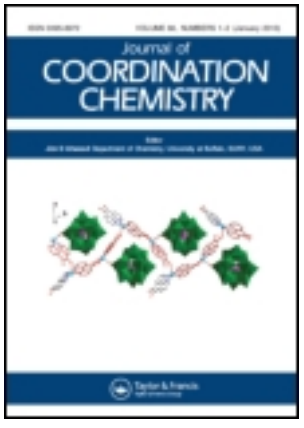

Journal of Coordination Chemistry
Publication details, including instructions for authors and subscription information:
http://www.tandfonline.com/loi/gcoo20

Syntheses and crystal structures of phthalato-, succinato-, maleato-, acetylenedicarboxylato-bridged [bis(2-pyridylcarbonyl)amide]copper(II) complexes

Wei Xu[a], Wei-Juan Pan[a] & Yue-Qing Zheng[a]
[a] Center of Applied Solid State Chemistry Research, Ningbo University, Ningbo, PR China
Accepted author version posted online: 14 Nov 2013.Published online: 10 Dec 2013.

To cite this article: Wei Xu, Wei-Juan Pan & Yue-Qing Zheng (2013) Syntheses and crystal structures of phthalato-, succinato-, maleato-, acetylenedicarboxylato-bridged [bis(2-pyridylcarbonyl)amide]copper(II) complexes, Journal of Coordination Chemistry, 66:24, 4415-4429, DOI: 10.1080/00958972.2013.862789

To link to this article: http://dx.doi.org/10.1080/00958972.2013.862789

Journal of Coordination Chemistry, 2013
Vol. 66, No. 24, 4415–4429, http://dx.doi.org/10.1080/00958972.2013.862789

Syntheses and crystal structures of phthalato-, succinato-, maleato-, acetylenedicarboxylato-bridged [bis (2-pyridylcarbonyl)amide]copper(II) complexes

WEI XU, WEI-JUAN PAN and YUE-QING ZHENG*

Center of Applied Solid State Chemistry Research, Ningbo University, Ningbo, PR China

(*Received 2 May 2013; accepted 17 October 2013*)

Self-assemblies of the 2,4,6-tris(2-pyridyl)-1,3,5-triazine (tptz) and $Cu(OH)_2$ in the presence of dicarboxylate ligands yielded four new complexes, $[Cu_4(bpca)_4(L1)_2(H_2O)_2]\cdot 5H_2O$ (**1**), $[Cu_2(bpca)_2(L2)(H_2O)_2]\cdot 2H_2O$ (**2**), $[Cu_2(bpca)_2(L3)(H_2O)_2]\cdot H_2O$ (**3**), and $[Cu_2(bpca)_2(L4)(H_2O)_2]\cdot 3H_2O$ (**4**) (bpca = bis(2-pyridylcarbonyl)amide anion, H_2L1 = phthalic acid, H_2L2 = succinic acid, H_2L3 = maleic acid, H_2L4 = acetylenedicarboxylic acid). Their structures were determined by single-crystal X-ray diffraction analyzes and further characterized by IR spectra and thermogravimetric analyzes. The five-coordinate Cu ions in **1** are bridged by phthalate to form 1-D chains, which are assembled into 3-D frameworks by extensive hydrogen bonds. Compounds **2**–**4** possess similar structures, built up of $[Cu_2(bpca)_2(L)(H_2O)_2]$ (L = L2 for **2**, L3 for **3**, L4 for **4**) and lattice molecules. The 3-D frameworks of **2**–**4** are completed by hydrogen bond interactions.

Keywords: Cu(II) complexes; Crystal structures; Bpca; Dicarboxylic

1. Introduction

Research on supramolecular chemistry [1–3] exploits rational design of metal-organic hybrid complexes via self-assembly of metal ions and various multifunctional ligands by noncovalent interactions. These weak interactions are important in stabilizing molecules like proteins and DNA, and arranging the structural units inside the crystal lattice [4]. Noncovalent intermolecular forces include classical hydrogen bonds and π–π stacking [5–11]. Hence, choices of multidentate ligands play an important role in design of metal-organic hybrid complexes [12–15]. Among those ligands, bis(2-pyridylcarbonyl)amidate (bpca) is widely used to construct homo- and heterometallic complexes [16–20]. Mononuclear $[M(bpca)_2]$ is an effective 'complex ligand', prepared by reaction of multidentate bpca with M. $[M(bpca)_2]$ is a bis-bidentate ligand with four C=O groups to form multi-metal-centered heteropolynuclear complexes, which show interesting magnetic behavior induced by direct or indirect M–M′ interactions [21–23]. The bpca could be obtained by reaction *in situ* from 2,4,6-tris(2-pyridyl)-1,3,5-triazine (tptz) [24, 25], which will hydrolyze in the presence of Cu^{2+} under mild conditions [26] or concentrated mineral acids with temperature above 150 °C [27]. Preliminary studies in our laboratory indicated that reaction of Cu^{2+}, tptz, or

*Corresponding author. Email: zhengcm@nbu.edu.cn

different dicarboxylic acid in methanol-water at room temperature afforded different hydrolytic products [28]. Little attention has been paid to related copper(II) complexes combining bpca and dicarboxylic anions [29, 30]. Here, we report the syntheses, structural characterizations, and thermal stability analyzes of four dicarboxylate-bridged [bis(2-pyridylcarbonyl)amide]copper(II) complexes, $[Cu_4(bpca)_4(L1)_2(H_2O)_2]\cdot 5H_2O$ (**1**), $[Cu_2(bpca)_2(L2)(H_2O)_2]\cdot 2H_2O$ (**2**), $[Cu_2(bpca)_2(L3)(H_2O)_2]\cdot H_2O$ (**3**), and $[Cu_2(bpca)_2(L4)(H_2O)_2]\cdot 3H_2O$ (**4**) (bpca = bis(2-pyridylcarbonyl)amide anion, H_2L1 = phthalic acid, H_2L2 = succinic acid, H_2L3 = maleic acid, H_2L4 = acetylenedicarboxylic acid).

2. Experimental

2.1. *Materials and physical methods*

All chemicals of reagent grade were commercially available and used without purification. Powder X-ray diffraction (PXRD) measurements were carried out with a Bruker D8 Focus X-ray diffractometer using a Cu target (λ = 1.54056 Å) and a Ni filter at room temperature with the range of 2θ between 5° and 50°. Single-crystal data were collected with a Rigaku R-Axis Rapid IP X-ray diffractometer using a Mo target (λ = 0.71073 Å). Infrared spectra were recorded from 4000–400 cm^{-1} using KBr pellets with an FTIR 8900 spectrometer. Thermogravimetric measurements were performed under a flow of nitrogen from room temperature to 820 °C at a heating rate of 10 °C min^{-1} using a Seiko thermal gravimetric (TG/DTA) 6300 apparatus. Temperature-dependent magnetic susceptibility was determined with a Quantum Design SQUID magnetometer (Quantum Design Model MPMS-7) from 2–300 K with an applied field of 1 kOe.

2.2. *Synthesis*

2.2.1. Synthesis of $[Cu_4(bpca)_4(L1)_2(H_2O)_2]\cdot 5H_2O$ (1). NaOH (2.0 mL, 1 M) was dropwise added to an aqueous solution of 0.172 g (1.0 mM) $CuCl_2\cdot 2H_2O$ to obtain blue precipitate, which was then centrifuged and washed with double-distilled water five times. The fresh precipitate was subsequently added to a stirred solution of 0.312 g (1.0 mM) tptz and 0.166 g (1.0 mM) phthalic acid in 20 mL CH_3OH/H_2O (1 : 1 v/v). The mixture was further stirred for half an hour and filtered off, the green filtrate (pH 4.74) was maintained at room temperature and blue crystals were formed three days later. Yield: 42% based on the initial $CuCl_2\cdot 2H_2O$. The phase purity of the crystalline product was confirmed by comparing experimental PXRD pattern with the corresponding one simulated on the basis of single-crystal data (figure 1). IR (KBr, cm^{-1}): 3421 w, 1710 s, 1589 ms, 1568 w, 1446 w, 1342 s, 1294 w, 1251 w, 1028 w, 759 m, 706 m, 653 w, 632 m.

2.2.2. Synthesis of $[Cu_2(bpca)_2(L2)(H_2O)_2]\cdot 2H_2O$ (2). A similar procedure with **1** was followed to prepare **2** except that 0.118 g (1.0 mM) succinic acid was used in place of phthalic acid. The resulting solution (pH 4.74) was kept at room temperature, and slow evaporation for one month afforded blue needle crystals. Yield: 45% based on the initial $CuCl_2\cdot 2H_2O$. The powder XRD pattern of the compound matches well with that simulated on the basis of single-crystal data (figure 1). IR (KBr, cm^{-1}): 3481 m, 1703 s, 1585 ms, 1392 m, 1356 s, 1298 m, 1226 w, 1026 w, 765 m, 707 m, 690 w, 632 m.

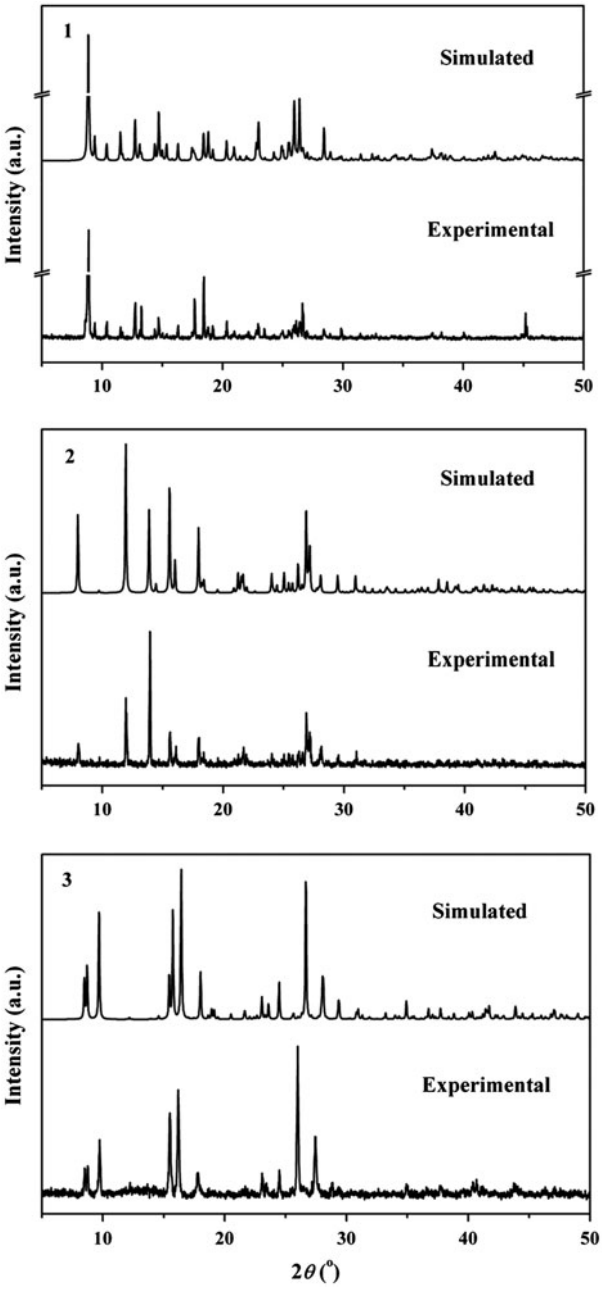

Figure 1. Experimental and simulated PXRD patterns of **1**, **2** and **3**.

2.2.3. Synthesis of $[Cu_2(bpca)_2(L3)(H_2O)_2]\cdot H_2O$ (3). **3** was prepared analogously to **1** except phthalic acid was changed with 0.116 g (1.0 mM) maleic acid. Blue crystals were obtained from the filtrate (pH 6.58) by slow evaporation after standing one month at room temperature. Yield: 70% based on the initial $CuCl_2\cdot 2H_2O$. The phase purity of the product

was checked according to powder X-ray pattern compared with the simulated PXRD based on single-crystal data (figure 1). IR (KBr, cm^{-1}): 3483 m, 1716 s, 1624 w, 1600 s , 1425 m, 1450 s, 1294 m, 1276 w, 1036 m, 762 m, 702 w, 655 w, 633 m.

2.2.4. Synthesis of $[Cu_2(bpca)_2(L4)(H_2O)_2]\cdot 3H_2O$ (4). **4** was synthesized in the same manner as **1** except that 0.114 g (1.0 mM) acetylenedicarboxylic acid was used in place of phthalic acid. The resulting solution (pH 6.08) was kept at room temperature, and slow evaporation for two weeks afforded blue crystals. Yield: 4% based on the initial $CuCl_2\cdot 2H_2O$. IR (KBr, cm^{-1}): 3506 w, 1716 vs, 1635 m, 1604 m, 1361 s, 1332 m, 1290 w, 1026 w, 761 m, 702 m, 673 m.

2.3. *X-ray crystallography*

Single-crystal diffraction data were collected at 295 K. Crystals were selected under a polarizing microscope and fixed with epoxy cement on respective fine glass fibers, which were then mounted on a Rigaku R-axis Rapid IP X-ray diffractometer with graphite-monochromated Mo-$K\alpha$ radiation (λ = 0.71073 Å). The data were corrected for *Lp* and absorption effects. Direct methods employing SHELXS-97 [31] gave the initial positions for some non-hydrogen atoms, and the subsequent difference Fourier syntheses using SHELXL-97 [32] resulted in initial positions for the rest of the non-hydrogen atoms. The structures were solved by direct methods and all non-hydrogen atoms were refined on F^2 anisotropically by full-matrix least-squares methods. After several cycles of refinement, hydrogens were located in calculated positions assigned a fixed isotropic displacement parameter at 1.2 times the equivalent isotropic U of the atoms to which they were attached, and allowed to ride on their respective parent, with 100% occupancy. Hydrogens of water were placed in the difference Fourier map. The key crystallographic information is summarized in table 1 and the main data of bond distances and bond angles are given in tables 2–5.

3. Results and discussion

3.1. *Description of the crystal structures*

The copper(II)-assisted hydrolysis of tptz in mild conditions afford the highly stable mononuclear complexes, which include $[Cu(bpca)]^+$ building block [33]. In mononuclear complexes, such as $[Cu(bpca)(H_2O)_2]NO_3\cdot 2H_2O$ [34], the Cu is square pyramidally coordinated by tridentate bpca groups and two coordinated waters. In **1–4**, one or two coordinated waters are replaced by different dicarboxylate anions, which bridge to form dinuclear complexes (scheme 1).

3.1.1. $[Cu_4(bpca)_4(L1)_2(H_2O)_2]\cdot 5H_2O$ (1). Compound **1** consists of 1-D chains $[Cu_2(bpca)_2(phthalato)_{2/2}(H_2O)]$ and lattice waters. The crystallographically independent Cu(1) and Cu(2) exhibit a distorted pyramidal surrounding, with trigonality parameter τ of 0.14 for Cu(1) and 0.10 for Cu(2) (τ = 0 and 1 for ideal square pyramid and trigonal bipyramid, respectively) [35]. The distorted square-pyramidal environment of Cu(1) has three N of a bpca, one O from phthalate and one O at the apex of the pyramid from a different

Table 1. Crystal data and structure refinement for **1–4**.

Compounds	**1**	**2**	**3**	**4**
Empirical formula	$C_{64}H_{54}Cu_4N_{12}O_{23}$	$C_{28}H_{28}Cu_2N_6O_{12}$	$C_{28}H_{24}Cu_2N_6O_{11}$	$C_{28}H_{26}Cu_2N_6O_{13}$
Formula mass	1613.35	767.64	747.61	781.63
Crystal system	Monoclinic	Monoclinic	Orthorhombic	Monoclinic
Description	Blue platelet	Blue needle	Blue block	Blue block
Crystal size (mm)	0.41 × 0.20 × 0.11	0.35 × 0.12 × 0.08	0.42 × 0.40 × 0.24	0.38 × 0.37 × 0.30
Temperature (K)	295(2)	295(2)	295(2)	295(2)
Space group	*C*2/*c*	$P2_1/n$	*Pbcn*	*C*2/*c*
a (Å)	42.820(9)	6.891(1)	6.861(1)	13.510(3)
b (Å)	7.820(2)	22.137(4)	20.293(4)	15.902(3)
c (Å)	20.118(4)	10.354(2)	20.834(4)	15.110(3)
β (°)	110.59(3)	105.81(3)		110.20(3)
Volume (Å^3)	6306(2)	1519.7(5)	2825(1)	3047(1)
Z	4	2	4	4
D_{Calcd} (g cm^{-3})	1.699	1.678	1.758	1.704
F (000)	3288	784	1520	1592
μ (mm^{-1})	1.425	1.475	1.582	1.476
Reflections collected	30,308	14,746	19,761	11,729
Unique reflections (R_{int})	7208 (0.0367)	3446 (0.0495)	2478 (0.0293)	2672 (0.0234)
Data, restraints, parameters	5742, 10, 486	2572, 6, 229	2202, 5, 223	2461, 7, 234
R_1, wR_2 [$I \geq 2\sigma(I)$][a]	0.0353, 0.0826	0.0396, 0.0852	0.0566, 0.1500	0.0328, 0.0913
R_1, wR_2 (all data)[a]	0.0494, 0.0880	0.0611, 0.0933	0.0609, 0.1543	0.0359, 0.0964
Goodness-of-fit on F^2	1.044	1.017	1.028	1.139
$\delta\rho_{max}$, $\delta\rho_{min}$ (e Å^{-3})	0.414, −0.326	0.527, −0.514	1.945, −0.914	0.439, −0.687

[a]$R_1 = \Sigma(||F_o|-|F_c||)/\Sigma|F_o|$, $wR_2 = [\Sigma w(F_o^2-F_c^2)^2/\Sigma w(F_o^2)^2]^{1/2}$, $w = [\sigma^2(F_o^2) + (aP)^2 + bP]^{-1}$ where $P = (F_o^2 + 2F_c^2)/3$. For **1**: $a = 0.0964$, $b = 5.9892$. For **2**: $a = 0.0429$, $b = 0.8497$. For **3**: $a = 0.0.0964$, $b = 5.9892$. For **4**: $a = 0.0537$, $b = 4.3405$.

Table 2. Selected interatomic distances (Å) and angles (°) for **1**.[a]

Cu(1)–O(6)$^{\#1}$	1.959(2)	Cu(1)–N(3)	2.003(2)	Cu(2)–N(5)	1.937(2)
Cu(1)–O(8)	2.300(2)	Cu(2)–O(7)	1.966(2)	Cu(2)–N(6)	1.993(2)
Cu(1)–N(1)	2.000(2)	Cu(2)–O(9)	2.317(2)		
Cu(1)–N(2)	1.940(2)	Cu(2)–N(4)	2.025(2)		
O(6)$^{\#1}$–Cu(1)–O(8)	89.16(7)	N(1)–Cu(1)–N(2)	81.86(8)	O(9)–Cu(2)–N(4)	88.37(9)
O(6)$^{\#1}$–Cu(1)–N(1)	96.45(8)	N(1)–Cu(1)–N(3)	163.01(8)	O(9)–Cu(2)–N(5)	93.27(8)
O(6)$^{\#1}$–Cu(1)–N(2)	163.13(8)	N(2)–Cu(1)–N(3)	81.40(8)	O(9)–Cu(2)–N(6)	104.74(8)
O(6)$^{\#1}$–Cu(1)–N(3)	100.42(8)	O(7)–Cu(2)–O(9)	86.55(7)	N(4)–Cu(2)–N(5)	81.73(8)
O(8)–Cu(1)–N(1)	90.36(7)	O(7)–Cu(2)–N(4)	99.40(7)	N(4)–Cu(2)–N(6)	159.26(8)
O(8)–Cu(1)–N(2)	107.59(8)	O(7)–Cu(2)–N(5)	178.84(8)	N(5)–Cu(2)–N(6)	81.53(8)
O(8)–Cu(1)–N(3)	91.95(7)	O(7)–Cu(2)–N(6)	97.40(8)		
Hydrogen bonding contacts					
D–H	*d*(D–H)	*d*(H···A)	∠(D–H···A)	*d*(D–H···A)	A
O(9)–H(9A)	0.83	2.07	146	2.794	O(11)$^{\#2}$
O(9)–H(9B)	0.82	2.10	149	2.835	O(4)$^{\#3}$
O(9)–H(9B)	0.82	2.38	132	2.988	O(3)$^{\#3}$
O(10)–H(10A)	0.81	2.54	130	3.125	O(2)
O(11)–H(11A)	0.82	2.00	167	2.804	O(7)$^{\#1}$
O(11)–H(11B)	0.82	2.03	163	2.831	O(12)
O(12)–H(12A)	0.82	2.14	162	2.935	O(1)$^{\#4}$
O(12)–H(12B)	0.85	1.95	172	2.797	O(6)$^{\#1}$

[a]Symmetry transformations used to generate equivalent atoms: #1 = *x*, *y* – 1, *z*; #2 = *x*, *y* + 1, *z*; #3 = –*x* + 1/2, *y* + 1/2, −*z* + 1/2; #4 = *x*, −*y* + 1, *z* − 1/2.

phthalate (figure 2(top)). The basal bond lengths are 1.940(2)–2.003(2) Å, while the axial Cu(1)–O(8) bond length is 2.300(2) Å (table 2). The geometry of Cu(2) is similar with Cu(1), coordinated by three N of another bpca, one O from phathalate and one O from an

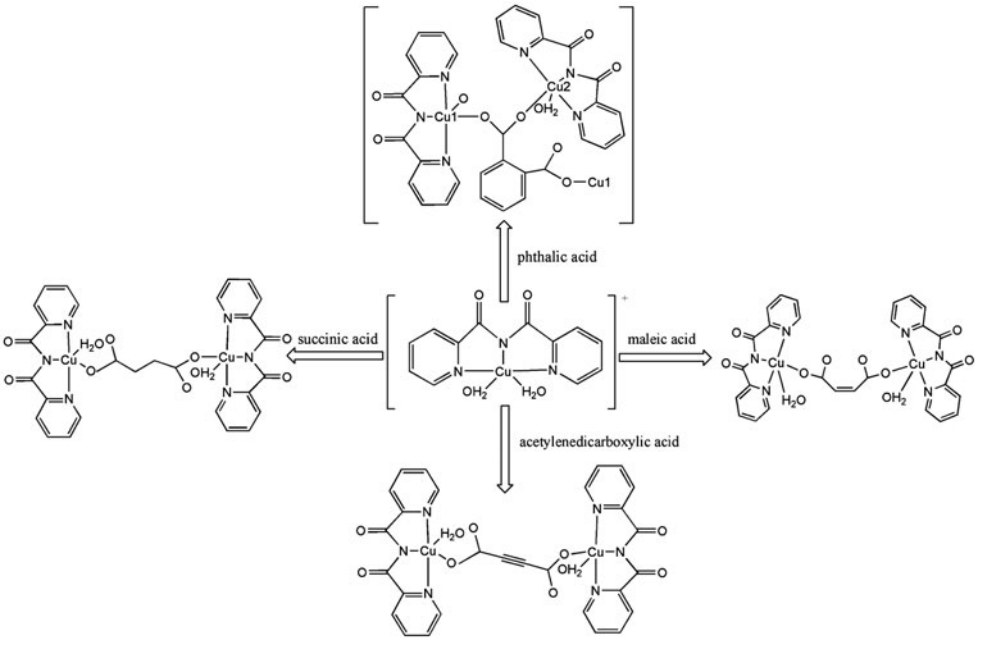

Scheme 1. Overview of the method for syntheses of **1–4**.

axial water. The basal bond lengths vary from 1.937(2) to 2.025(2) Å with the axial bond d(Cu(2)–O(9)) = 2.317(2) Å significantly longer than the basal bonds. In phthalate, the bidentate and monodentate carboxylates deviate from the mean plane of benzene with dihedral angles of 52.06° and 48.49°, respectively. Each phthalate bridges three Cu ions to generate 1-D supramolecular chains [$Cu_2(bpca)_2(phthalato)_2/_2(H_2O)$] parallel to [010] direction. The resulting 1-D chains are coupled into double chains through O–H···O hydrogen bonds between coordinated water and carbonyl O (O(4)) and (O(3)) of a bpca (figure 2(bottom)). Furthermore, the double chains are interlinked into 2-D layers perpendicular to the [001] direction by weak C–H···O interactions. The lattice waters are sandwiched between 2-D layers, which are connected into a 3-D network via extensive interlayer hydrogen bonds.

3.1.2. [$Cu_2(bpca)_2(L2)(H_2O)_2$]·$2H_2O$ (2). Compound **2** is built up of [$Cu_2(bpca)_2$(succinato)$(H_2O)_2$] and lattice waters. Within the complex Cu is square pyramidal, coordinated by three N and two O. The τ value is 0.13 indicating the slight distortion of the square pyramid. The water is situated at the apical position and the basal plane is defined by carboxylate oxygen of succinate and three nitrogens of a bpca (figure 3(top)). The apical Cu–O bond distance is 2.267(2) Å and the equatorial bond lengths range from 1.934(2) to 2.019(2) Å (table 3). Succinate exhibits *anti* conformational coordination bridging two Cu ions to form the dinuclear [$Cu_2(bpca)_2$(succinato)$(H_2O)_2$]. Each molecule connects with four neighboring molecules with two types of hydrogen bonds, O(1)···O(4)$^{\#1}$ and O(1)···O(5)$^{\#1}$ (table 3) to form 2-D layers perpendicular to [101] direction (figure 3(bottom)). The resulting 2-D layers are stabilized by hydrogen bonds between lattice water and O(2)$^{\#3}$ and O(5). Due to interlayer hydrogen bonds O(1)···O(3)$^{\#2}$, the 2-D layers are assembled into a 3-D supramolecular architecture.

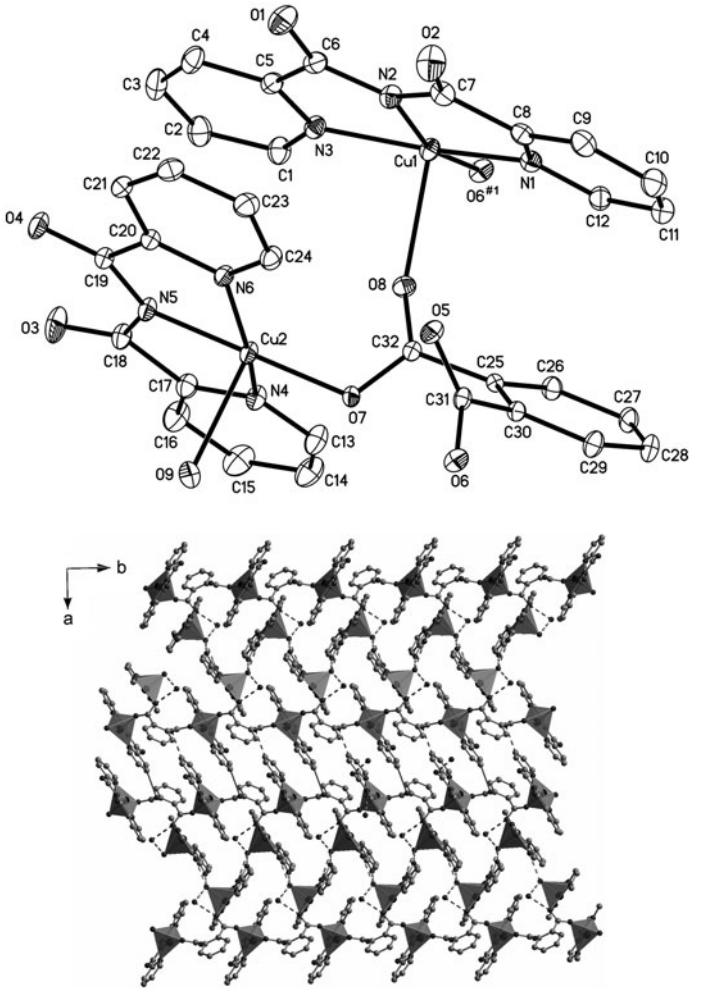

Figure 2. (Top) ORTEP view of **1** (45% thermal ellipsoids) showing the atom-labeling scheme. Hydrogens and lattice waters are omitted for clarity. Symmetry code #1: x, $y - 1$, z; (bottom) supramolecular layer of **1** formed from 1-D chain $^{1}_{\infty}[Cu_2(bpca)_2(phthalato)_{2/2}(H_2O)]$ by hydrogen bonds indicated by dashed lines.

3.1.3. $[Cu_2(bpca)_2(L3)(H_2O)_2]\cdot H_2O$ (3). Compound **3** consists of $[Cu_2(bpca)_2(maleato)(H_2O)_2]$ and lattice waters. Cu ions are in distorted square pyramidal coordination (τ value: 0.14) with the equatorial plane defined by three N of bpca and one O of maleate and the apical position occupied by one water (figure 4(top)). The equatorial bond distances range from 1.934(3) to 2.008(3) Å and the apical Cu–O bond length is 2.257(4) Å (table 4). The maleate is bidentate bridging two Cu ions to form dinuclear $[Cu_2(bpca)_2(maleato)(H_2O)_2]$. The C=C double bond distance is 1.264(8) Å, representative of C=C [36]. The hydrogen bond between water O(1) and uncoordinated carboxylate ($d(O(1)\cdots O(3)^{\#2})$ = 2.832 Å, $\angle(O(1)\text{-}H\cdots O(3)^{\#2})$ = 171°) (table 4) connects $[Cu_2(bpca)_2(maleato)(H_2O)_2]$ to form 1-D supramolecule chains extending along the [100] direction. The resulting 1-D chains are assembled into 2-D layers perpendicular to [010] (figure 4(bottom)) by interchain hydrogen

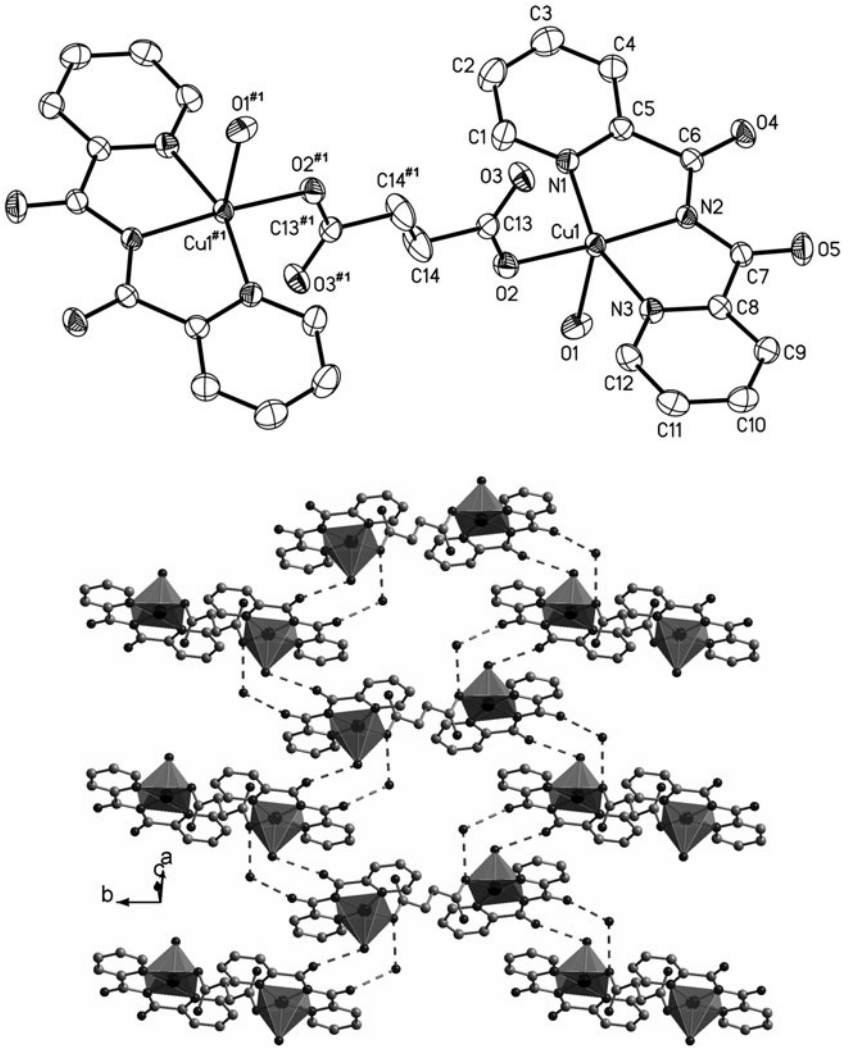

Figure 3. (Top) ORTEP view of **2** (45% thermal ellipsoids) showing the atom-labeling scheme. Hydrogens and lattice waters are omitted for clarity. Symmetry code #1: $-x + 1, -y, -z + 1$; (bottom) 2-D supramolecular layer of **2** formed by hydrogen indicated by dashed lines.

bonds between coordinated water O(1) and carbonyl O $O(4)^{\#1}$ of a bpca (d(O(1)–H···O $(4)^{\#1}$) = 2.832 Å, ∠(O(5)–H···$O(4)^{\#1}$) = 145°) as shown in figure 4(bottom). The lattice waters O(6) in the 2-D layer donate hydrogen bonds to coordinated carboxylate O(2) with d(O(6)–H···O(2)) = 2.894 Å, ∠(O(6)–H···O(2)) = 172°, stabilizing the 2-D layer. Furthermore, C–H···O hydrogen bonds play an important role in formation of the 3-D network.

3.1.4. $[Cu_2(bpca)_2(L4)(H_2O)_2]\cdot 3H_2O$ (4). The structure of **4** is similar to that of **2** and **3** consisting of $[Cu_2(bpca)_2$(acetylenedicarboxylato)$(H_2O)_2]$ and lattice waters. The Cu shows distorted square-pyramidal coordination with the τ value being 0.14, with the basal plane

Table 3. Selected interatomic distances (Å) and angles (°) for **2**.[a]

Cu(1)–O(1)	2.267(2)	Cu(1)–N(1)	2.011(3)	Cu(1)–N(3)	2.019(2)
Cu(1)–O(2)	1.934(2)	Cu(1)–N(2)	1.942(2)		
O(1)–Cu(1)–O(2)	90.12(9)	O(2)–Cu(1)–N(1)	98.10(9)	N(1)–Cu(1)–N(3)	161.31(9)
O(1)–Cu(1)–N(1)	98.30(9)	O(2)–Cu(1)–N(2)	172.67(9)	N(2)–Cu(1)–N(3)	81.58(9)
O(1)–Cu(1)–N(2)	97.16(9)	O(2)–Cu(1)–N(3)	81.58(9)		
O(1)–Cu(1)–N(3)	92.11(9)	N(1)–Cu(1)–N(2)	81.74(9)		
Hydrogen bonding contacts					
D–H	*d*(D–H)	*d*(H···A)	∠(D–H···A)	*d*(D–H···A)	A
O(1)–H(1A)	0.81	2.18	153	2.925	O(4)$^{\#1}$
O(1)–H(1A)	0.81	2.42	129	3.006	O(5)$^{\#1}$
O(1)–H(1B)	0.80	2.00	172	2.791	O(3)$^{\#2}$
O(6)–H(6A)	0.82	2.08	161	2.866	O(2)$^{\#3}$
O(6)–H(6B)	0.83	2.09	159	2.877	O(5)

[a]Symmetry transformations used to generate equivalent atoms: #1 = $x-1/2, -y+1/2, z-1/2$; #2 = $x-1, y, z$; #3 = $x+1/2, -y+1/2, z+1/2$.

completed by three N of bpca [Cu–N(1), 2.018(2); Cu–N(2), 1.994(2); Cu–N(3), 2.014(2) Å] and one O from acetylenedicarboxylate [Cu–O(3), 1.973(2) Å]. The apical position is occupied by O(1) of water [Cu–O(1), 2.236(2) Å] (figure 5(top), table 5). The dinuclear $[Cu_2(bpca)_2(acetylenedicarboxylato)(H_2O)_2]$ are obtained by bridging of acetylenedicarboxylate, in which the C≡C triple bond distance (1.185(5) Å) is normal [37]. As shown in figure 5(bottom), a 1-D chain structure is formed along the *c* axis through four types of intermolecular hydrogen bonds, O(1)···O(6)$^{\#1}$, O(1)···O(3)$^{\#2}$, O(6)···O(2)$^{\#3}$, and O(7)···O(1) (table 5). The resulting 1-D chains are assembled into 2-D layers perpendicular to [010] by two types of interchain hydrogen bonds, O(6)···O(4) and O(6)···O(5) (figure 5(bottom)). Weak C–H···O hydrogen bonds interlink the 2-D layers to complete the 3-D network of the compound.

3.1.5. Structural comparison of 1–4. Although the synthetic methods of **1–4** are similar, their final structures are different. Complexes **2–4** display centrosymmetric-dumbbell structures. The succinate, maleate, and acetylenedicarboxylate anions in **2–4** behave similarly. They bridge two $[Cu(H_2O)(bpca)]$ moieties with terminal carboxylate to form dinuclear $[Cu_2(bpca)_2L(H_2O)_2]$. The phthalate in **1** is coordinated to three Cu ions with μ_2-η^2:η^1 chelating and μ_1-η^1:η^0 bridging mode, one carboxylate chelates one Cu and one chelating carboxyl O bonds to the other Cu, while the other carboxylate bridges the third Cu. Through phthalate, [Cu(bpca)] moieties are interlinked into $[Cu_2(bpca)_2(phthalato)_2/_2(H_2O)]$ chains with chelating bpca distributed on both sides. In these complexes, extensive hydrogen-bonding interactions play an important role in the supramolecular assembly of the dinuclear motifs or polymeric chains into 3-D networks.

3.1.6. Structural comparison of other Cu(II)-bpca containing complexes. The bpca (Hbpca = bis(2-pyridylcarbonyl)amidate) is capable of being a bridging ligand via N_3 and O_2 sites which have different coordination abilities. The structures of bpca-containing copper(II) mononuclear complexes show that bpca is tridentate through its three nitrogens occupying three of the four equatorial positions around copper. In the cases where a 1 : 1 (Cu(II)/bpca) molar ratio occurs, the remaining equatorial site and the axial positions around copper are filled by either solvent and/or counterions [18, 25, 34, 38–42]. With anions or

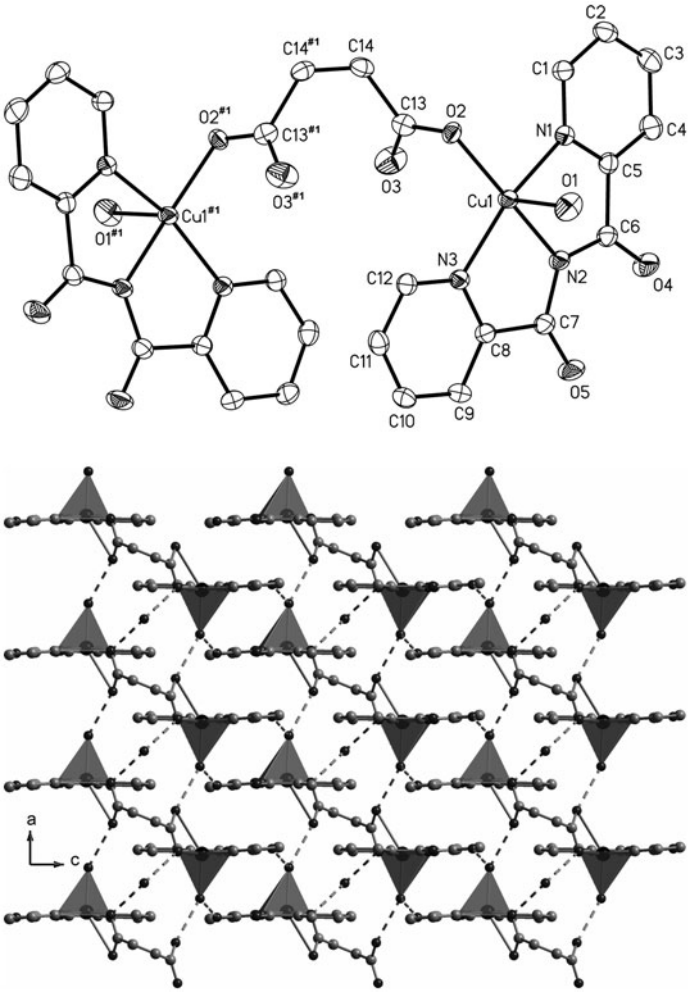

Figure 4. (Top) ORTEP view of **3** (45% thermal ellipsoids) showing the atom-labeling scheme. Hydrogens and lattice waters are omitted for clarity. Symmetry code #1: $-x + 2$, y, $-z + 1/2$; (bottom) supramolecular layer of **3** formed from $[Cu_2(bpca)_2(L3)(H_2O)_2]$ by hydrogen bonds indicated by dashed lines.

Table 4. Selected interatomic distances (Å) and angles (°) for **3**.[a]

Cu(1)–O(1)	2.257(4)	Cu(1)–N(1)	2.008(3)	Cu(1)–N(3)	2.005(3)
Cu(1)–O(2)	1.953(3)	Cu(1)–N(2)	1.934(3)		
O(1)–Cu(1)–O(2)	93.4(1)	O(2)–Cu(1)–N(1)	94.0(1)	N(1)–Cu(1)–N(3)	162.7(1)
O(1)–Cu(1)–N(1)	97.0(1)	O(2)–Cu(1)–N(2)	171.4(1)	N(2)–Cu(1)–N(3)	81.9(1)
O(1)–Cu(1)–N(2)	94.6(1)	O(2)–Cu(1)–N(3)	101.0(1)		
O(1)–Cu(1)–N(3)	90.7(1)	N(1)–Cu(1)–N(2)	82.1(1)		
Hydrogen bonding contacts					
D–H	*d*(D–H)	*d*(H···A)	∠(D–H···A)	*d*(D–H···A)	A
O(1)–H(1A)	0.85	2.09	145	2.832	O(4)$^{\#1}$
O(1)–H(1A)	0.85	2.45	136	3.128	O(5)$^{\#1}$
O(1)–H(1B)	0.85	1.87	171	2.713	O(3)$^{\#2}$
O(6)–H(6A)	0.83	2.07	172	2.894	O(2)

[a]Symmetry transformations used to generate equivalent atoms: #1 = $-x + 1$, $-y$, $1 - z$; #2 = $x - 1$, y, z.

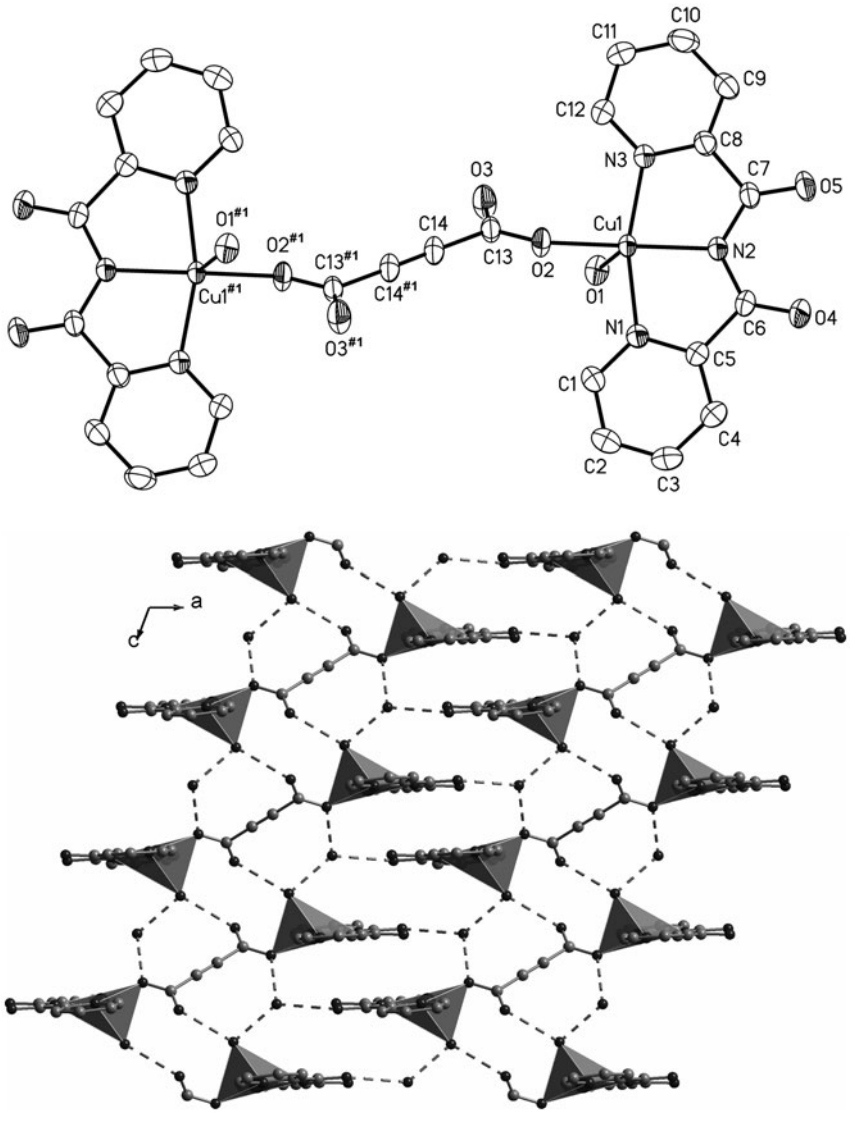

Figure 5. (Top) ORTEP view of **4** (45% thermal ellipsoids) showing the atom-labeling scheme. Hydrogens and lattice waters are omitted for clarity. Symmetry code #1: $-x$, $-y + 1$, $-z + 2$; (bottom) supramolecular layer of **4** formed from $[Cu_2(bpca)_2(L4)(H_2O)_2]$ by hydrogen bonds indicated by dashed lines.

neutral ligands as bridging ligands oligomeric and polymeric species have been obtained, like the dinuclear compounds $[Cu_2(bpca)_2(H_2O)_n(X)]$ (X = 4,4′-bipyridine, trans-1,2-bis(4-pyridyl)ethylene [43], CrO_4^-, SO_4^{2-} [44], $C_2O_4^{2-}$ [45], MoO_4^{2-}, WO_4^{2-} [46], squarato [47], isophthalato [48], sebacato [30], phthalato, succinato, maleato, acetylenedicarboxylato dianions [this work]), the trinuclear complex $\{[Cu(bpca)(H_2O)]_2[Cu(1,2\text{-dithiocroconate})_2]\}\cdot 2H_2O$ [49], the 1-D polymers [Cu(bpca)X] (X = CN^-, N_3^- [50], tricyanomethanide [51]), and $[Cu_3(bpca)_2(bpy)_3(NO_3)_4]\cdot H_2O$ [43]. Moreover, the $[Cu(bpca)(H_2O)_2]^+$ building

Table 5. Selected interatomic distances (Å) and angles (°) for **4**.[a]

Cu(1)–O(1)	2.236(2)	Cu(1)–N(1)	2.018(2)	Cu(1)–N(3)	2.014(2)
Cu(1)–O(3)	1.973(2)	Cu(1)–N(2)	1.944(2)		
O(1)–Cu(1)–O(2)	93.25(8)	O(2)–Cu(1)–N(1)	93.08(8)	N(1)–Cu(1)–N(3)	163.34(9)
O(1)–Cu(1)–N(1)	91.87(8)	O(2)–Cu(1)–N(2)	157.90(9)	N(2)–Cu(1)–N(3)	81.86(8)
O(1)–Cu(1)–N(2)	108.26(9)	O(2)–Cu(1)–N(3)	102.25(8)		
O(1)–Cu(1)–N(3)	93.73(8)	N(1)–Cu(1)–N(2)	81.49(8)		
Hydrogen bonding contacts					
D–H	*d*(D–H)	*d*(H···A)	∠(D–H···A)	*d*(D–H···A)	A
O(1)–H(1A)	0.81	1.83	174	2.639	O(6)#1
O(1)–H(1B)	0.80	2.17	153	2.904	O(3)$^{\#2}$
O(6)–H(6A)	0.82	2.08	149	2.811	O(5)
O(6)–H(6A)	0.82	2.39	128	2.967	O(4)
O(6)–H(6B)	0.83	1.99	173	2.814	O(2)$^{\#3}$
O(7)–H(7A)	0.84	2.26	138	2.936	O(1)

[a]Symmetry transformations used to generate equivalent atoms: #1 = $-x + 1$, y, $-z + 3/2$; #2 = $-x$, y, $-z + 3/2$; #3 = $-x$, $-y + 1$, $-z + 2$.

block can also work as a bidentate donor through the two carbonyl groups of the ligand, as shown by the copper(II) 1-D polymer $[Cu(bpca)]ClO_4$ [50] and trinuclear complex $\{Cu(bpca)_2[Mn(hfac)_2]_2\}$ (Hhfac = hexafluoroacetylacetone) [52].

3.2. *Thermal stability analyzes*

To examine the thermal stabilities of these compounds, TG analyzes were carried out for **1–3** (figure 6). The TG curve of **1** shows two weight loss steps. The first weight loss is 8.95% from 35 to 130 °C, which corresponds to loss of coordinated and lattice water (Calcd: 8.92%), while the second weight loss corresponds to the removal of all organic components from 245 to 820 °C to yield CuO (Found: 20.08%; Calcd 19.71%).

For **2**, the weight loss of 9.68% at 60–170 °C agrees with liberation of coordinated and lattice water (Calcd value: 9.37%). The weight loss of 68.79% from 200 to 820 °C is slightly less than the calculated value 69.82% expected for bpca and succinate. The remaining weight (21.63%) is close to CuO (20.71%).

The TG curve of **3** exhibits two weight loss stages from 60 to 180 °C (7.58%) and 200–820 °C (71.14%). The first step corresponds to liberation of coordinated and lattice water (Calcd value: 7.22%), while the second step corresponds to release of all organic components (Calcd value: 71.42%). The residue of 21.28% is in agreement with the Calcd value for CuO (21.27%).

3.3. *Magnetic properties*

Only the magnetic properties of **1** have been measured; those of **2–4** were not investigated because of their mononuclear nature. The magnetic behavior of **1** in the form of the $\chi_m T$ and χ_m *versus* T plots is depicted in figure 7 (χ_m being the magnetic susceptibility per two Cu(II) ions). At 300 K, the $\chi_m T$ value is 0.68 $cm^3\ M^{-1}$ K, smaller than the spin-only value of 0.83 $cm^3\ M^{-1}$ K for two magnetically isolated spin doublets. The $\chi_m T$ value increases smoothly from 300 K on cooling, exhibiting a weak ferromagnetic interaction. The $\chi_m T$ gives a higher value of 0.837 $cm^3\ M^{-1}$ K at 14 K and decreases further to 0.827 $cm^3\ M^{-1}$ K at 4 K, and then it increases sharply, reaching a maximum of 0.853 $cm^3\ M^{-1}$ K at 2 K. The

decrease of $\chi_m T$ after 14 K in the curve of **1** is most likely due to zero-field splitting (D) and/or intermolecular interactions. The temperature-dependent magnetic susceptibility follows the Curie-Weiss law $\chi_m = C/(T - \theta)$, and the best fit of the χ_m *versus* T plot gives a Curie constant $C = 0.83(1)$ cm^3 M^{-1} K and the Weiss constant $\theta = 0.07(1)$, suggesting the presence of weak ferromagnetic interaction among Cu(II) ions.

The structure of **1** consists of dinuclear units where two equatorial sites of copper(II) are connected by an *anti-syn* carboxylate bridge, and these dinuclear units are further connected through hydrogen bonds. In the light of these features, we analyzed the magnetic data of **1** through the Bleaney-Bowers equation (equation (1)) [53] for two interacting spin doublets (the isotropic spin Hamiltonian being $\hat{H} = -J\hat{S}_1 \cdot \hat{S}_2$). Because only a weak magnetic interaction was expected in the molecular-field approximation as zJ', the measured magnetic susceptibility data were fitted to (equation (2)).

$$\chi_m = \frac{N\beta^2 g^2}{kT}\left[\frac{2\exp(-D/kT)}{1 + 2\exp(-D/kT) + \exp(-2J/kT)}\right] \quad (1)$$

$$\chi'_m = \frac{\chi_m}{1 - \chi_m(2zJ'/N\beta^2 g^2)} \quad (2)$$

The best-fit parameters are $g = 2.118(1)$, $J = 0.23(5)$ cm^{-1}, $zJ' = -0.05(4)$ cm^{-1} and $D = 0.08(2)$ cm^{-1}, with the agreement factor $R = 3.00 \times 10^{-5}$ ($\Sigma[(\chi_m)^{obs} - (\chi_m)^{calcd}]^2/[(\chi_m)^{obs}]^2$). The positive J corroborates ferromagnetic superexchange mechanism across the dinuclear copper(II) centers of **1**, and the negative zJ' clearly indicates the existence of very weak antiferromagnetic coupling between adjacent Cu(II) ions, consistent with the magnetic behavior.

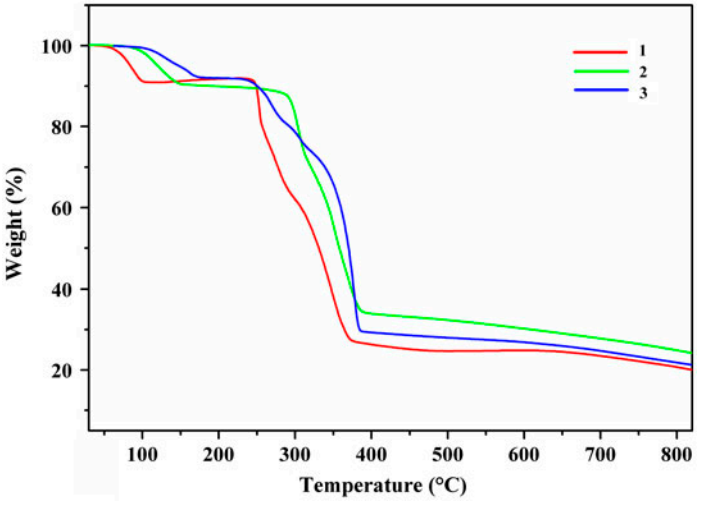

Figure 6. The TG curves of **1–3**.

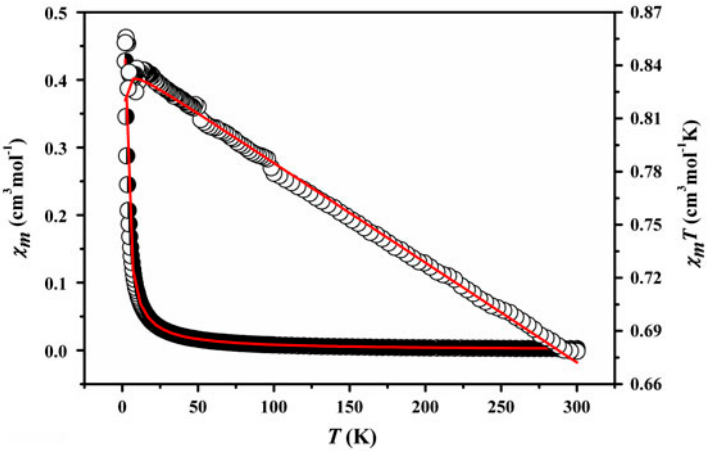

Figure 7. $\chi_m T$ and χ_m *vs.* T plots for **1**. Solid lines represent the best fits.

4. Conclusion

The combined use of tptz, $Cu(OH)_2$ and different dicarboxylic acids as bridging ligands afforded four [bis(2-pyridylcarbonyl)amide]copper(II) complexes. The syntheses of these compounds revealed that copper(II)-assisted hydrolysis of 2,4,6-tris(2-pyridyl)-1,3,5-triazine produced polynuclear copper(II) complexes in the presence of four-carbon chain dicarboxylic acids.

Supplementary material

Details on data collection and refinement, fractional atomic coordinates, anisotropic displacement parameters, and full list of bond lengths and angles are in CIF format. Crystallographic data for **1–4** deposited with the Cambridge Crystallographic Data Center, CCDC-736500, CCDC-736501, CCDC-936779, and CCDC-936780. [CCDC, 12 Union Road, Cambridge CB2 1EZ, UK; Fax: (44)1223–336-033; Email: deposit@ccdc.cam.ac.uk; website: http://www.ccdc.cam.ac.uk].

Funding

This project was sponsored by K.C. Wong Magna Fund in Ningbo University and supported by the Open Foundation from Application of Nonlinear Science and Technology in the Most Important Subject of Zhejiang [Grant number xkzl2006].

References

[1] J.W. Steed, J.L. Atwood. *Supramolecular Chemistry*, 2nd Edn, John Wiley & Sons, Chichester, (2009).
[2] S.H. Hsu, M.D. Yilmaz, D.N. Reinhoudt, A.H. Velders, J. Huskens. *Angew. Chem. Int. Ed.*, **52**, 714 (2013).
[3] B. Moulton, M.J. Zaworotko. *Chem. Rev.*, **101**, 1629 (2001).
[4] H.M. Yamamoto, J.I. Yamaura, R. Kato. *J. Am. Chem. Soc.*, **120**, 5905 (1998).
[5] Y.Y. Zhou, J. Li, L. Ling. *Angew. Chem. Int. Ed.*, **52**, 1452 (2013).

[6] S.T. Schneebeli, M. Kamenetska, Z.L. Cheng. *J. Am. Chem. Soc.*, **133**, 2136 (2011).
[7] M. Taddei, F. Costantino, R. Vivani, C. Sangregorio, L. Sorace, L. Castelli. *Cryst. Growth Des.*, **12**, 2327 (2012).
[8] H.W. Roesky, M. Andruh. *Coord. Chem. Rev.*, **236**, 91 (2003).
[9] C.C. Pradzynski, R.M. Forck, T. Zeuck, P. Slavíček, U. Buck. *Science*, **337**, 1529 (2012).
[10] A.M. Beatty. *Coord. Chem. Rev.*, **246**, 131 (2003).
[11] L. Infantes, J. Chisholm, S. Motherwell. *CrystEngComm*, **5**, 480 (2003).
[12] S. Kitagawa, R. Kitaura, S. Noro. *Angew. Chem. Int. Ed.*, **43**, 2334 (2004).
[13] M. O'Keeffe, O.M. Yaghi. *Chem. Rev.*, **112**, 675 (2012).
[14] J.J. Perry IV, J.A. Perman, M.J. Zaworotko. *Chem. Soc. Rev.*, **38**, 1400 (2009).
[15] Z.Z. Lu, R. Zhang, Y.Z. Li, Z.J. Guo, H.G. Zheng. *J. Am. Chem. Soc.*, **133**, 4172 (2011).
[16] T. Senapati, C. Pichon, R. Ababei, C. Mathoniere, R. Clerac. *Inorg. Chem.*, **51**, 3796 (2012).
[17] R. Sahu, V. Manivannan. *Inorg. Chim. Acta*, **363**, 4008 (2010).
[18] M. Ferbinteanu, T. Kajiwara, K.Y. Choi, H. Nojiri, A. Nakamoto, N. Kojima, F. Cimpoesu, Y. Fujimura, S. Takaishi, M. Yamashita. *J. Am. Chem. Soc.*, **128**, 9008 (2006).
[19] A. Kamiyama, T. Noguchi, T. Kajiwara, T. Ito. *Angew. Chem. Int. Ed.*, **39**, 3130 (2000).
[20] P. Paul, B. Tyagi, A.K. Bilakhiya, M.M. Bhadbhade, E. Suresh. *J. Chem. Soc., Dalton Trans.*, 2009 (1999).
[21] A. Kamiyama, T. Noguchi, T. Kajiwara, T. Ito. *CrystEngComm*., **5**, 231 (2003).
[22] T. Kajiwara, M. Nakano, Y. Kaneko, S. Takaishi, T. Ito, M. Yamashita, A. Igashira-Kamiyama, H. Nojiri, Y. Ono, N. Kojima. *J. Am. Chem. Soc.*, **127**, 10150 (2005).
[23] A.M. Madalan, K. Bernot, F. Pointillart, M. Andruh, A. Caneschi. *Eur. J. Inorg. Chem.*, **35**, 5533, (2007).
[24] P. Paul, B. Tyagi, M.B. Bhadbhade, E. Suresh. *J. Chem. Soc., Dalton Trans.*, 2273 (1997).
[25] J. Borrás, G. Alzuet, M. González-Álvarez, F. Estevan, B. Macías, M. Liu-González, A. Castiñeiras. *Polyhedron*, **26**, 5009 (2007).
[26] L.M. Toma, R. Lescouëzec, D. Cangussu, R. Llusar, J. Mata, S. Spey, J.A. Thomas, F. Lloret, M. Julve. *Inorg. Chem. Commun.*, **8**, 382 (2005).
[27] E.M. Smolin, L. Rapoport. *S-Triazines and Derivatives, Interscience*, p. 163, Interscience Publishers, New York (1959).
[28] Y.Q. Zheng, W. Xu, F. Lin, G.S. Fang. *J. Coord. Chem.*, **59**, 1825 (2006).
[29] J. Cano, D. De Munno, J.L. Sanz, R. Ruiz, F. Lloret, J. Faus, M. Julve. *An. Quim.*, **93**, 174 (1997).
[30] W. Xu, H.L. Zhu, J.L. Lin, Y.Q. Zheng. *J. Coord. Chem.*, **66**, 171 (2013).
[31] G.M. Sheldrick, *SHELXS-97, Program for Crystal Structure Solution*, University of Göttingen, Germany (1997).
[32] G.M. Sheldrick, *SHELXL-97, Program for Crystal Structure Refinement*, University of Göttingen, Germany (1997).
[33] D.C. Gomes, L.M. Toma, H.O. Stumpf, H. Adams, J.A. Thomas, F. Lloret, M. Julve. *Polyhedron*, **27**, 559 (2008).
[34] I. Castro, J. Faus, M. Julve, J.M. Amigó, J. Sletten, T. Debaerdemaeker. *J. Chem. Soc., Dalton Trans.*, 891 (1990).
[35] A.W. Addison, T.N. Rao, J. Reedijk, J. van Rijin, G.C. Verschoor. *J. Chem. Soc., Dalton Trans.*, 1349 (1984).
[36] K.L. Zhang, Y. Xu, J.G. Lin, X.Z. You. *J. Mol. Struct.*, **703**, 63 (2004).
[37] D. Visinescu, G.I. Pascu, M. Andruh, J. Magull, H.W. Roesky. *Inorg. Chim. Acta*, **340**, 201 (2002).
[38] J.V. Folgado, E. Martínez-Tamayo, A. Beltrán-Porter, D. Beltrán-Porter, A. Fuertes, C. Miravitlles. *Polyhedron*, **8**, 1077 (1989).
[39] B. Vangdal, J. Carranza, F. Lloret, M. Julve, J. Sletten. *J. Chem. Soc., Dalton Trans.*, 566 (2002).
[40] S.K. Padhi, V. Manivannan. *Inorg. Chem.*, **45**, 7994 (2006).
[41] J. Borras, G. Alzuet, M. Gonzalez-Alvarez, J.L. García-Giménez, B. Macías, M. Liu-Gonzalez. *Eur. J. Inorg. Chem.*, **6**, 822, (2007).
[42] X.P. Zhou, D. Li, S.L. Zheng, X. Zhang, T. Wu *Inorg Chem.*, **45**, 7119 (2006).
[43] L. Carlucci, G. Ciani, S. Maggini, D.M. Proserpio, R. Sessoli, F. Totti. *Inorg. Chim. Acta*, **376**, 538 (2011).
[44] M.L. Calatayud, I. Castro, J. Sletten, F. Lloret, M. Julve, *Inorg. Chim. Acta*, **300**, 846 (2000).
[45] I. Castro, J. Faus, M. Julve, M. Mollar, A. Monge, E. Gutierrez-Puebla. *Inorg. Chim. Acta*, **161**, 97 (1989).
[46] M.L. Liu, W. Gu, Z.P. Ma, P. Zhu, Y.Q. Gao, X. Liu. *J. Coord. Chem.*, **61**, 3476 (2008).
[47] I. Castro, J. Faus, Y. Journaux, J. Sletten. *J. Chem. Soc., Dalton Trans.*, 2533 (1991).
[48] J. Cano, G. De Munno, J.L. Sanz, R. Ruiz, F. Lloret, J. Faus, M. Julve. *An. Quim.*, **93**, 174 (1997).
[49] J. Sletten, M. Julve, F. Lloret, I. Castro, G. Seitz, K. Mann. *Inorg. Chim. Acta*, **250**, 219 (1996).
[50] H. Casellas, F. Costantino, A. Mandonnet, A. Caneschi, D. Gatteschi. *Inorg. Chim. Acta*, **358**, 177 (2005).
[51] D.C. de Castro Gomes, L.M. Toma, H.O. Stumpf, H. Adams, J.A. Thomas, F. Lloret, M. Julve. *Polyhedron*, 27, 559 (2008).
[52] A. Kamiyama, T. Noguchi, T. Kajiwara, T. Ito. *Inorg. Chem.*, **41**, 507 (2002).
[53] O. Kahn, *Molecular Magnetism*, p. 135–141, VCH, Weinheim (1993).